Fire Safety Journal 58 (2013) 1–14

Contents lists available at SciVerse ScienceDirect

Fire Safety Journal

journal homepage: www.elsevier.com/locate/firesaf

Determinations of the fire smoke layer height in a naturally ventilated room

Chi-ming Lai [a], Chien-Jung Chen [b], Ming-Ju Tsai [b], Meng-Han Tsai [c], Ta-Hui Lin [c,*]

[a] Department of Civil Engineering, National Cheng-Kung University, Taiwan
[b] Architecture and Building Research Institute, Ministry of Interior, Taiwan
[c] Department of Mechanical Engineering, National Cheng-Kung University, 1, University Road, Tainan City 701, Taiwan

ARTICLE INFO

Article history:
Received 11 April 2011
Received in revised form
1 August 2012
Accepted 26 January 2013

Keywords:
Fire
Natural ventilation
FDS
Smoke layer
N-percentage rule

ABSTRACT

According to the case-based reasoning of natural ventilation designs in recommended Green Buildings, an investigated model space was proposed in this study. FDS simulations and full-scale experiments were carried out to measure the impact of natural ventilation conditions and the installation of a natural ventilation shaft on smoke layer descent during different fire scenarios. The feasibility of using the *N*-percentage rule to determine the fire smoke layer height in a naturally ventilated space was also investigated.

In a non-fire room, the smoke descent curve determined from the FDS simulated temperatures is consistent with the experimentally measured temperatures and visual observation of the smoke layer. However, the thermocouples in the fire room are affected by direct burning and fire radiation, and the experimentally measured temperatures cannot be used to determine the smoke height. Under these conditions, FDS simulations can be used to compensate for the lack of experimental measurements. In fire scenarios without outdoor winds blowing into the building's interior, FDS simulations can reliably model the fire smoke layer height. When outdoor air blows into the interior, it causes the smoke layer temperature to become unstable. Thus, the temperature will not be thermally stratified, and the use of the *N*-percentage rule is not recommended.

1. Background information

Natural ventilation has many benefits, including reduced building energy consumption and improved indoor air quality (IAQ), so it has become an important part of Green Building design. Although natural ventilation design can create an interior airflow path, it may also have significant impacts on how room fires spread and how high-temperature gases and smoke flow during a fire. Therefore, the interaction and mutual relationship between natural ventilation design and fire safety are worth exploring.

1.1. Fire smoke exhaust can be considered during natural ventilation design

A building that possesses good natural ventilation necessarily features a considerable number of vertical penetrations and horizontal interconnecting spaces. However, fire safety is jointly achieved through passive design with fire prevention construction, active fire suppression systems and active fire safety management. Thus, designs featuring natural ventilation sometimes conflict with designing for maximum fire safety (especially when considering a passive design with fire prevention construction) or regulations.

Chow and Chow [1] pointed out that in Hong Kong, some Green Building designs are unable to satisfy the needs of fire safety regulations. For example, the indoor complex space, double-layered building skin, too much natural ventilation (paths and amount), high atrium, etc. To address these design concerns (Green Building design vs. fire safety), the author suggests using a fire engineering approach to strike an appropriate balance between the two design considerations. Chen et al. [2] analyzed the impact of outdoor wind velocity on room fire smoke flow and discovered that smoke will be guided by the ventilation system when the wind velocity is large enough or when the strength of the fire source is comparatively smaller than the wind velocity. In other words, if the natural ventilation is properly designed, the smoke in the early fire stage can be guided outdoors following the natural ventilation path and the evacuation time can be increased. A study by Short et al. [3] showed that in a building designed for natural ventilation, satisfying the compartment requirements of fire safety regulations is bound to increase the cost through additional fire doors, fire dampers, etc. Those facilities will adversely affect the daily performance of natural ventilation. Using a mechanical ventilation facility as a smoke exhaust will not only increase cost, it will also conflict with the value-engineering concepts of natural ventilation design.

Since 1998, many green buildings in Hong Kong have employed high atrium designs to achieve better natural ventilation performance, obtain more daylight and create a better indoor thermal environment. However, Hung and Chow [4] argued that many high atrium designs are unable to meet fire safety regulations. Chow [5]

* Corresponding author. Tel.: +886 6 2757575x62167; fax: +886 6 2352973.
E-mail address: thlin@mail.ncku.edu.tw (T.-H. Lin).

0379-7112/$ - see front matter © 2013 Elsevier Ltd. All rights reserved.
http://dx.doi.org/10.1016/j.firesaf.2013.01.015

performed a fire disaster scenario analysis and stated that a fire located under the atrium at a hypermarket would not be controlled by sprinklers because the sprinkling action at the top level would suppress the smoke layer, causing it to move to lower floors and accumulate.

1.2. FDS applications

Numerical simulations are often used to explore complicated full-scale fires, and simulation software has developed and progressed rapidly. However, due to an insufficient material database and incomplete physical and chemical simulation models of material burning and pyrolysis, there is still room for significant improvement in the field of numerical simulation. Full-scale fire experiments can be used to examine the accuracy of numerical results and improve their precision. Many numerical simulation software packages are available, and FDS (Fire Dynamics Simulator) [6] from NIST (National Institute of Standards and Technology), is widely used among fire groups to simulate building fires. FDS has been used in a large number of studies and applications in recent years, including smoke and flow characteristics in fire scenarios [7–10], room fire simulations [11–12], arson fire reconstruction [13] and firefighting modeling [14].

FDS is widely used with various parameters in fire simulations and provides valuable information about smoke movement, local temperatures, gas concentrations and velocities. However, there are some limitations to this type of model. For example, FDS only deals with the combustion of single gaseous fuels, which leads to poor predictions in situations involving multiple fuels. Some work at the University of Edinburgh [15,16] has shown that FDS does not accurately model fires in small under-ventilated compartments. The general conclusion is that the modeling of realistic enclosed fires must be supplemented by experimental fire test measurements directly related to the event under study.

In this study, FDS simulations and full-scale experiments were used to investigate the impact of natural ventilation on fire smoke exhaust. As there are a number of key components of natural ventilation design, this study focuses on the impact of natural ventilation operational status and the use of a natural ventilation shaft on fire smoke exhaust. FDS simulations were used to compensate for the lack of experimental detail.

2. Full-scale experiment

After analyzing a number of natural ventilation designs of Green Building protocols, this study has inferred a research subject as illustrated in the dotted area shown in Fig. 1. The main target of which was the vertical natural ventilation shaft and spaces connected by this shaft. The illustrative research subject came in geometrical alike space, including two rooms with a connecting space of a natural ventilation shaft, and a room without a natural ventilation shaft but with a direct connecting door to the outside.

Such research subject looked like a two-story building, but was not necessarily low in level, but could also represent a high floor at a certain area. The two rooms on the first floor were called Room1 and Room2. The Room1 measures 5.4 m in interior length, 5.4 m in width and 3.0 m in ceiling height and Room2 has 3.6 m in interior length, 5.4 m in width and 3.0 m in ceiling height. The two 2.0 m (H) × 0.8 m (W) doors on the first floor were called Door1 (outdoor door) and Door2 (interior door), the vent on the first floor was called Vent1. All rooms have (horizontal) ceiling which is made of a light rigid frame and gypsum boards.

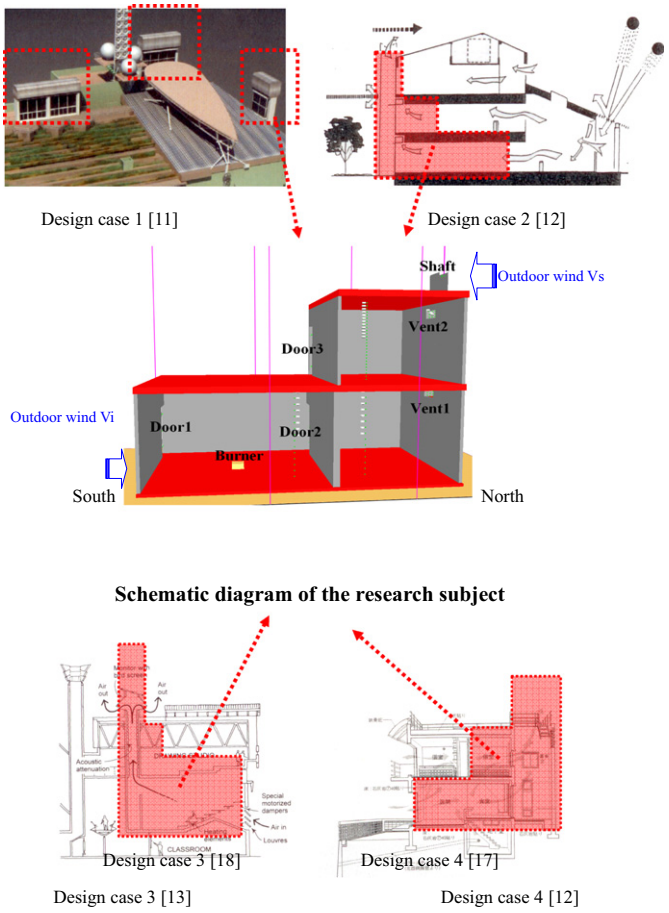

Fig. 1. Development of the research subject.

The natural ventilation shaft was sized in accordance with the Building Design and Construction Code Article 43 (ventilation) and Article 44 (structure of natural ventilation facility) of the Taiwanese Building Technical Regulations. The cross-sectional area of the natural ventilation shaft was 30 cm × 40 cm, the size of indoor Vent1 size was set to 30 cm × 40 cm, and the vent was installed 20 cm below the ceiling in the middle of the wall.

Opening windows or doors are commonly used for natural ventilation purpose. The installation of a natural ventilation shaft is only considered in spaces with particular characteristics or spaces requiring outdoor environment connection. In order to achieve natural ventilation performance, this study designed a single indoor airflow route, used outdoor Door1 as the opening needed for natural ventilation and used a natural ventilation shaft to guide the airflow outdoors. Door2 and Door3 were always fully open and closed respectively. Therefore, the overall ventilation pathway was designed as: Door1 → Room1 → Door2 → Room2 → Vent1 → Shaft. In daily use, this ventilation route design was designed for natural ventilation. However, in the event of a fire, the impact of this ventilation route on fire smoke flow was the focus of observation in this study.

A full-scale experimental space was constructed at the outdoor experimental site at ABRI (Architecture & Building Research Institute), Ministry of the Interior, Taiwan, as shown in Fig. 2. The space was constructed in accordance with the design concepts and dimensions of the research subject shown in Fig. 1. The eastern side of this experimental space was constructed using glass to allow the smoke flow and smoke layer descent to be observed.

Thermocouple trees were installed in the experimental space to measure air temperatures. Each thermocouple tree consisted of

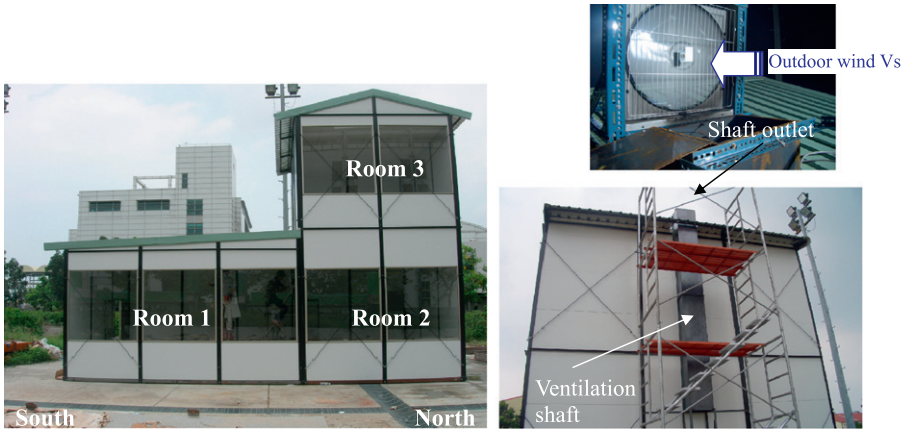

Fig. 2. Full-scale experimental model space.

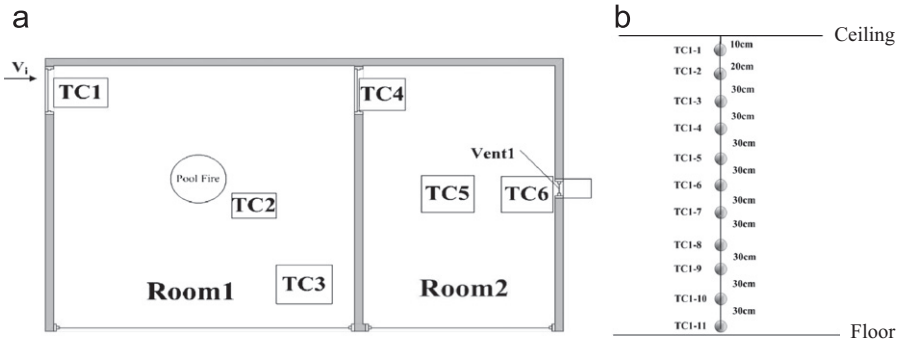

Fig. 3. (a) Thermocouple tree locations and (b) thermocouple tree (unit: cm).

Table 1
Experimental scenarios.

No.	Fire source (50 kW)	Vent1	V_i (m/s)	V_s (m/s)	Outdoor environment condition
0-1-C	Room1	Closed	0	0	For comparison
0-2-C	Room2	Closed	0	0	For comparison
0-1	Room1	Open	0	0	Stagnant wind condition
0-2	Room2	Open	0	0	Stagnant wind condition
1-1	Room1	Open	0	5, N	Mimicking the winter season
1-2	Room2	Open	0	5, N	Mimicking the winter season
2-1	Room1	Open	1, S	5, S	Mimicking the summer season
2-2	Room2	Open	1, S	5, S	Mimicking the summer season

a set of type K thermocouples tied vertically onto a thin iron chain which was attached to the ceiling. A fan was installed by the side of the exit of the vertical natural ventilation shaft and could blow over the exit to mimic outdoor wind. The simulated wind velocity could be changed in different experimental scenarios. The structures and locations of the thermocouple trees are shown in Fig. 3, and a camera was set up outside of the glass panels to film the smoke flow.

A 26 cm-diameter oil pan was used inside the model space to generate flame and dense smoke. The relationship of the oil pan diameter and fuel mass loss rate, proposed by Babrauskas [17], was used to estimate the oil mass loss rate: $\dot{m}''=0.055$ kg/m^2 s and $k\beta=2.1$. The fuel used was unleaded gasoline with a heat generation mass of $\Delta H=43.7$ MJ/kg. The heat release rate was known to be 50 kW through calculation. The main purpose of this study was to explore the impact of natural ventilation conditions and a natural ventilation shaft on fire smoke flow. A total of eight fire scenarios were set up in this study and are listed in Table 1.

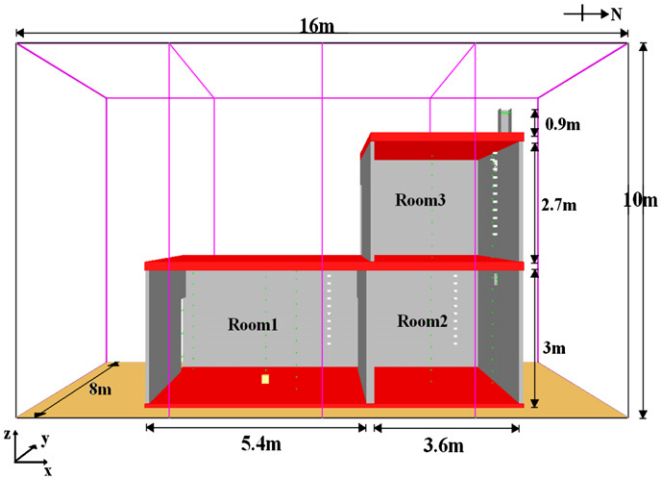

Fig. 4. Schematic diagram of the simulation domain.

Experiment No. 0-1-C was a scenario with no natural ventilation shaft. The purpose of this experiment was to understand fire smoke flows when a fire was initiated in Room1, which was directly connected to outdoors. Scenario No. 0-2-C was used to investigate fire smoke flow when the fire was initiated inside Room2, which had a natural ventilation shaft, but Vent1 was closed.

Table 2
Used parameters during the FDS simulations.

Objects	Setting	Properties
Ceiling	'brick'	'Default'
Wall	'brick'	'Default'
Floor	'brick'	'Default'
Shaft	'metal'	'Iron' Density=7870 (kg/m^3); Conductivity=80.2 (W/m/K); SPECIFIC_HEAT=0.447 (kJ/kg/K)
Burner	'GASOLINE'	C=8.0; H=18.0; SOOT_YIELD=0.1 HEAT_OF_COMBUSTION=44,400 (kJ/kg)

In experiments No. 0-1 and No. 0-2, Vent1 in Room2 was opened. These experiments were compared with No. 0-1-C and No. 0-2-C to determine the impact of natural ventilation shaft operation on fire smoke layer descent.

In experiments No. 1-1 and No. 1-2, the fan installed by the side of the natural ventilation shaft outlet was operated to mimic an outdoor wind velocity of 5 m/s. The purpose of this experiment was to determine the impact of a winter monsoon (conventional northern wind in Taiwan) blowing at 5 m/s on the model space.

The purpose of the two experiments No. 2-1 and No. 2-2 was to explore the fire smoke flow when the summer monsoon (conventional south wind) was blowing at 5 m/s toward the experimental model space. Meanwhile, Door1 had been set with a fan, with a fan speed of which was set up in reference to FDS simulation results. The honeycomb was not used and thus it is possible that the experimental turbulence intensity was high. The software FDS [6] was used to simulate the south wind blowing at 5 m/s from the outside toward the experimental model space. The wind velocity as a function of height above ground is assumed to follow the power law. The exponent is set to be 0.15, which is suitable for the experimental site. The simulation results showed that the wind velocity that blew into the interior was about 0.8 m/s to 0.9 m/s.

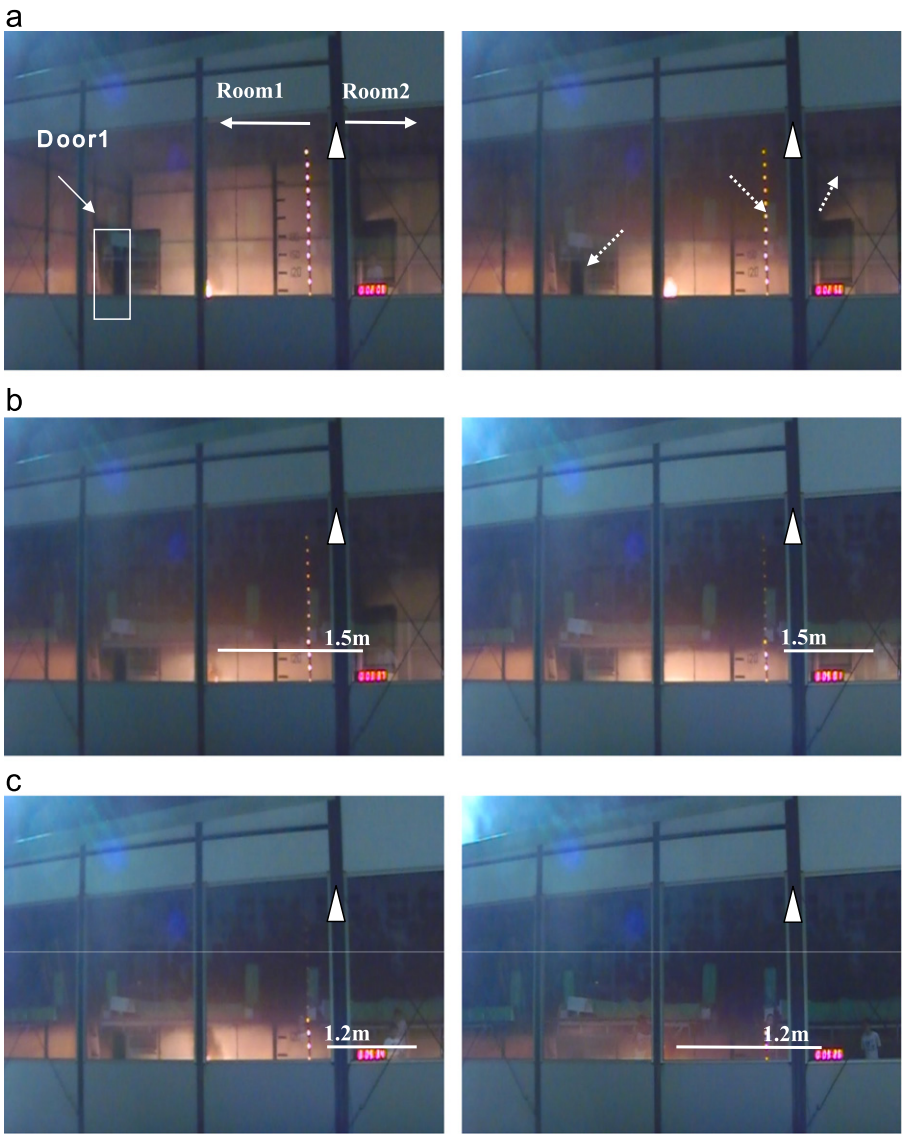

Fig. 5. Experimental photo of Experiment No. 0-1-C. (a) 2'08" (128"), (ignition) and 2'58" (178") (Room1→Room2), (b) 3'37" (187"), (1.5m, Room1) and 5'01" (301"), (1.5m, Room2), (c) 5'35" (335"), (1.2m, Room2) and 9'25" (565"), (1.2m, Room1).

In reference to the FDS simulation results and for convenience sake, the outside fan at Door1 was set at a wind velocity of 1 m/s blowing toward the interior during the two experimental scenarios.

The experimental procedures were:

(a) The fans and openings were set in accordance with the experimental scenarios shown in Table 1.
(b) The oil pan was filled with 1 l of unleaded gasoline.
(c) The timer was switched on.
(d) The indoor airflow was allowed to stabilize for 2 min.
(e) The oil pan was ignited. Smoke flow development and smoke layer accumulation were observed. The experiment ended after 10 min (600 s).
(f) The interior fan was used to blow out the smoke and allow the room temperature to decrease.
(g) The indoor smoke was allowed to disperse for 30 min.
(h) The next experiment was then conducted.

During the experiment period (October, 2009), the average outdoor air temperature was 27 °C; the highest daytime temperature was 34 °C; the lowest nighttime temperature was

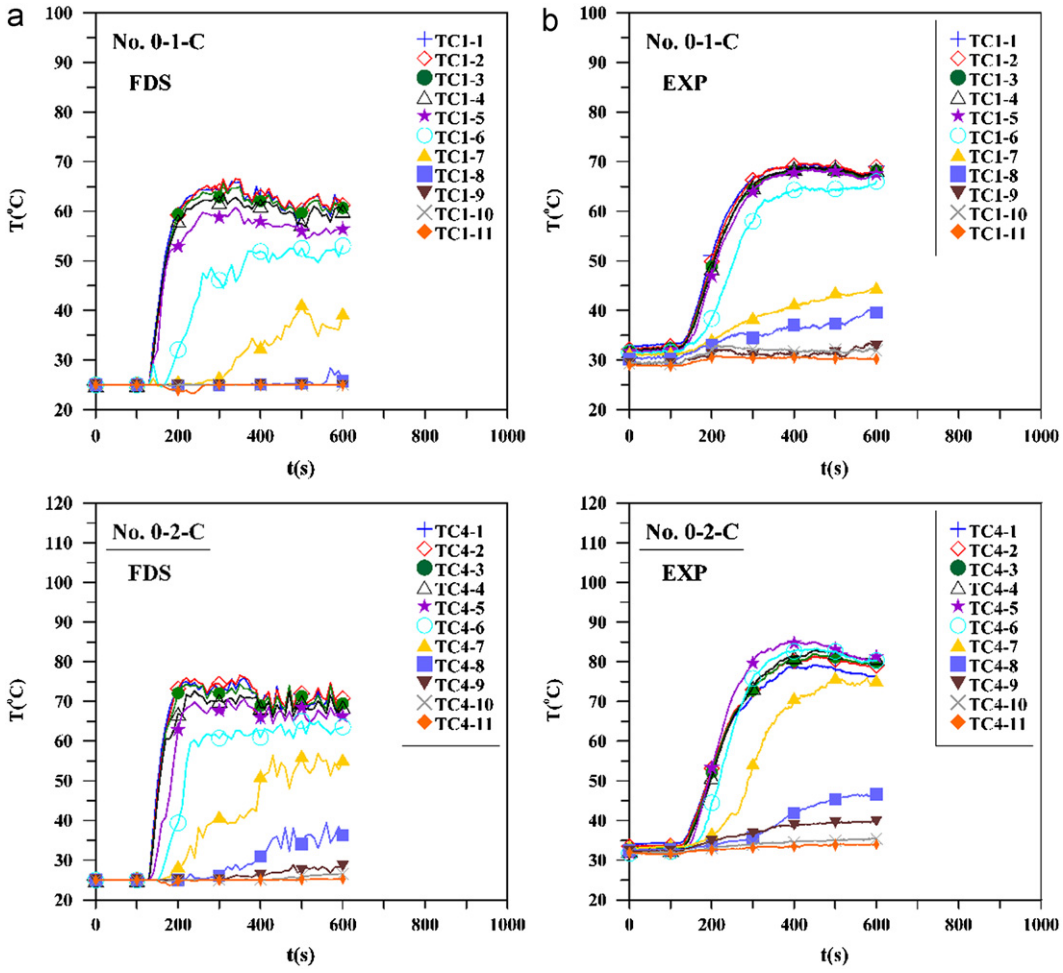

Fig. 6. A comparison of FDS simulation results with experimental data. (a) FDS simulations and (b) Experiments.

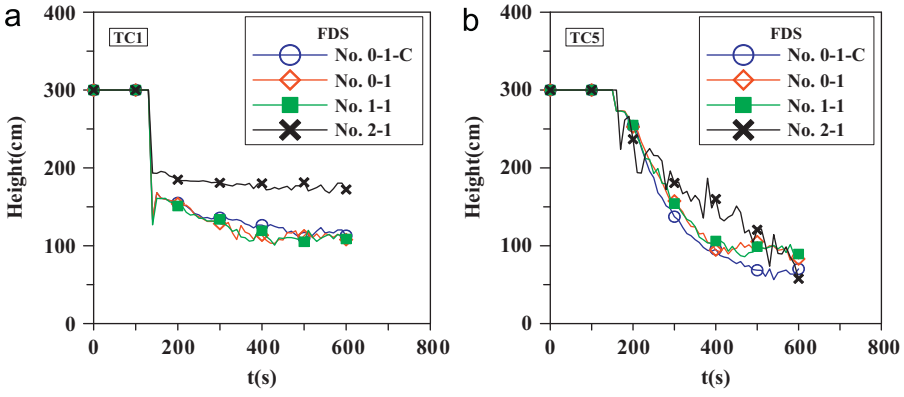

Fig. 7. FDS simulations of smoke layer descent when the fire source was in Room1. (a) Smoke layers in Room1 and (b) Smoke layers in Room2.

20.2 °C; the relative humidity was 71%; the outdoor air velocity was between 0.5 and 1.2 m/s.

Currently, the common methods used in defining the smoke layer boundary are: (1) shading percentage, (2) bulb luminosity, and (3) *N*-percentage rule. Among them, the *N*-percentage rule involves using the detected air temperatures to calculate the smoke boundary position. Such formula was proposed by Copper et al. [18] in 1982, but they did not define the setting criteria on the *N* value. That thesis utilized $N=10\%$, 15% and 20% to verify the accuracy of the *N*-percentage rule, and among them, $N=10\%$ was the most compliant to the smoke layer descending of that experiment. In NFPA 92B [19], it has also mentioned that this method can be used to calculate smoke layer height, but its content has only suggested to determine the bottom of the smoke layer with an *N* value of 80–90%, but does not tell the specific method to obtain the appropriate *N* value.

While in the studies done by other scholars, different *N* values were set to accommodate different fire scenes. Yi et al. [20] had set the *N* value of the smoke layer height as 30%. This indicates that *N* can be set according to the experimental scenarios. There is yet a setting criterion on *N* value. While this study was conducting the experiment No. 0-1-C, the smoke layer position was visually observed by a number of observers at the same time. After comparison, we discovered that the *N* value set at 30% was the most appropriate at the setup scene. Therefore, *N*-30% was used by this study as the *N*-percentage rule to calculate the air temperature

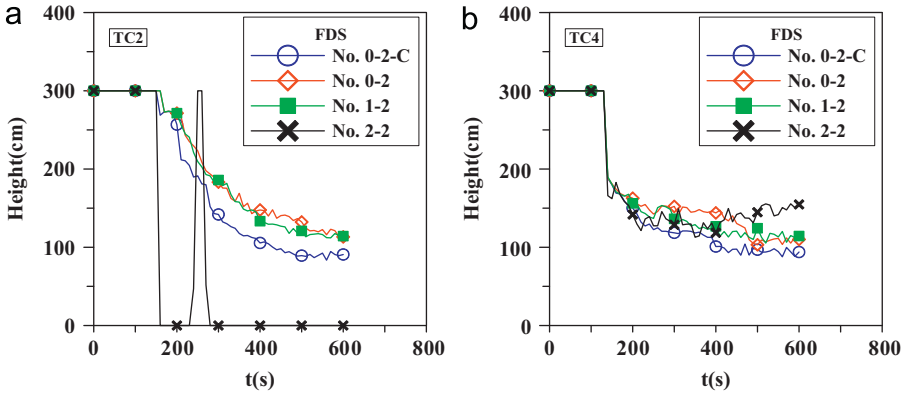

Fig. 8. FDS simulations of smoke layer descent when the fire source was in Room2. (a) Smoke layers in Room1 and (b) Smoke layers in Room2.

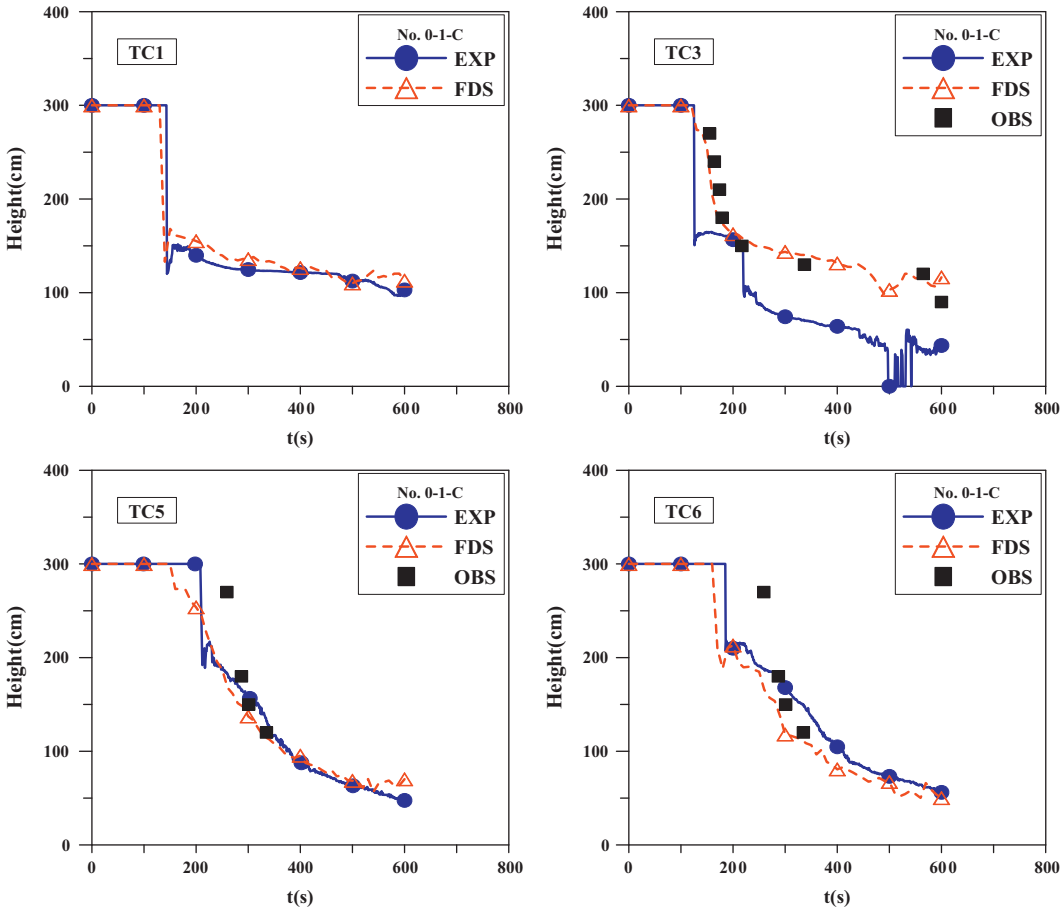

Fig. 9. A comparison of smoke layer descent in No. 0-1-C.

changes in the fire scenario as the smoke layer height. In addition, the smoke layer height was also observed by the naked eye.

3. Numerical simulation

The simulation domain was set to mimic the experimental model room (Figs. 1 and 2), as shown in Fig. 4. The dimensions of the simulated geometry were a length (x direction) of 16 m, width (y direction) of 8 m and height (z direction) of 10 m. The length of the airflow wake and the boundary layer thickness could be considered separately in the simulation.

The interior layout was the same as that of the experiment, which is shown in Fig. 1. A burner of area 0.2 m × 0.2 m was placed in the room to simulate the fire source. The fire source could be placed in the middle of Room1 or Room2 to meet the different experimental scenarios, and the heat release rate was set to 50 kW to match the calculated rate.

The CFD package used in this study was FDS 5.2.3, developed by NIST [6]. It is well known that the size of the calculation grid can directly affect the simulation results. Ma and Quintiere [21] used FDS to simulate axially symmetric flames. A characteristic length, defined as the ratio of the grid size to the characteristic flame length, is incorporated. A characteristic length of around 0.05 has been shown to produce the best simulation results for the flame length. McGrattan et al. [22] and Kwon [23] showed that, by considering experimental conditions and computing time, a grid size of 0.1 m is acceptable for determining the characteristic flame length.

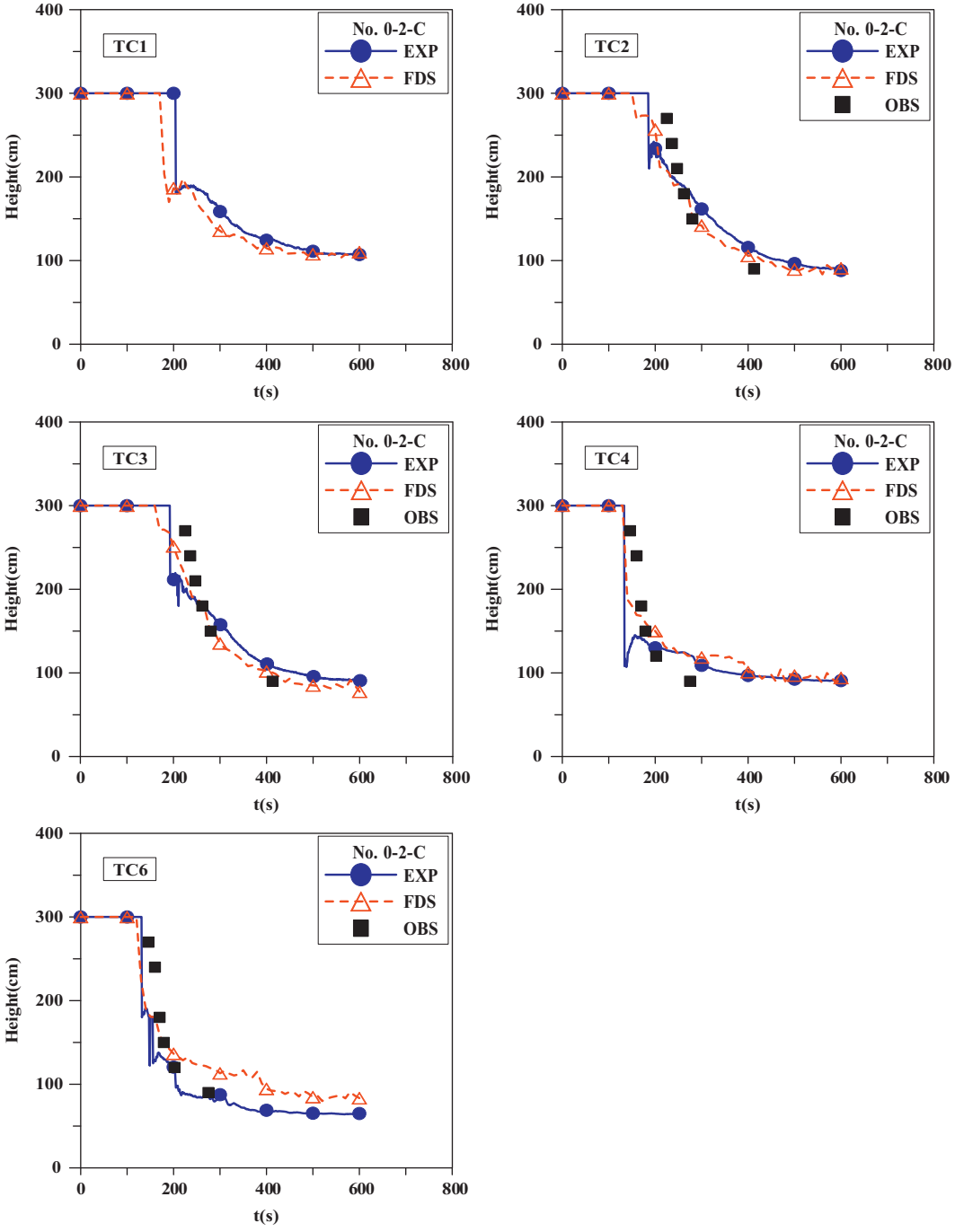

Fig. 10. A comparison of smoke layer descent in No. 0-2-C.

According to these studies, the grid size in our study was determined by the following equation proposed by Ma and Quintiere [21].

$$z^* = \max(\delta_x,\delta_y,\delta_z)/(\dot{Q}/\rho_\infty C_p T_\infty g^{1/2})^{2/5} \quad (1)$$

where $\dot{Q}$ is the heat release rate (kW), ρ_∞, C_p, and T_∞ are properties of ambient air. According to their study, Z^* of 0.05 corresponds to an optimal grid size for best resolution of fire plume. Therefore, we use grid size (δ_i) of 0.1 m corresponding to $Z^*=0.05$ in the numerical simulation. The grid size was set to 0.1 m to provide sufficient accuracy in a reasonable computational time, and the simulated space was cut into four sub-spaces and solved by a parallel computational approach.

The geometry of the openings and layout of the fixed fire load were identical to the full-scale experimental test. Since the width and height of the computational domain will influence the output, before formal simulation, the size of computational domain has been determined by observing the air flow pattern. The computational domain width of wind direction is extended by 3 and 4 m in x-direction. After comparison, it is found that wind field begins to stabilize when the wind field width is extended in x-direction, so the computational domain width is defined as 16 m. Meanwhile, the computational domain width of y-direction can also be defined by the same method, and the result is 8 m. The height of simulated space is 3–5.7 m. In this research the computational domain heights in z-direction are set to be 8, 10 and 15 m. After test it is found that the wind field begins to stabilize at the height between 10 and 15 m. Thus, in this study the computational domain is conservatively set as 16 m × 8 m × 10 m, as shown in Fig. 4. A total of 320,000 grids were constructed.

Because the interior surfaces did not burn, the FDS default value 'brick', which does not take part in material combustion, was adopted as the wall material. The ventilation shaft material was set to iron to conform to the actual situation, and the fuel was set as octane to match the actual fuel supply. The physical and chemical properties of the fuel were set to reflect its actual properties. The parameters used during the numerical simulations are listed in Table 2.

The outdoor wind velocity profile incident on the model space was set according to the commonly used power law:

$$v = v_s\left(\frac{h}{h_0}\right)^n \quad (2)$$

where v refers to the wind velocity at height h, and v_s refers to the wind velocity at the nominal height h_0 (10 m from the ground). v_s was set to 5 m/s, n is related to the ground surface roughness and atmospheric stability and was set to 0.15 in our model, which is the typical value for the experiment site (rural area) and the wind was set to blow from the south or north to match the experimental setup. A total of 8 fire scenarios were simulated, as shown in Table 1, and each was compared with the corresponding experimental results.

4. Results and discussion

4.1. Fire smoke progress and temperature changes

The setup of Experiment No. 0-1-C is shown in Fig. 5. Fire smoke flow with no natural ventilation shaft was modeled by closing the natural ventilation shaft and placing the fire source in Room1.

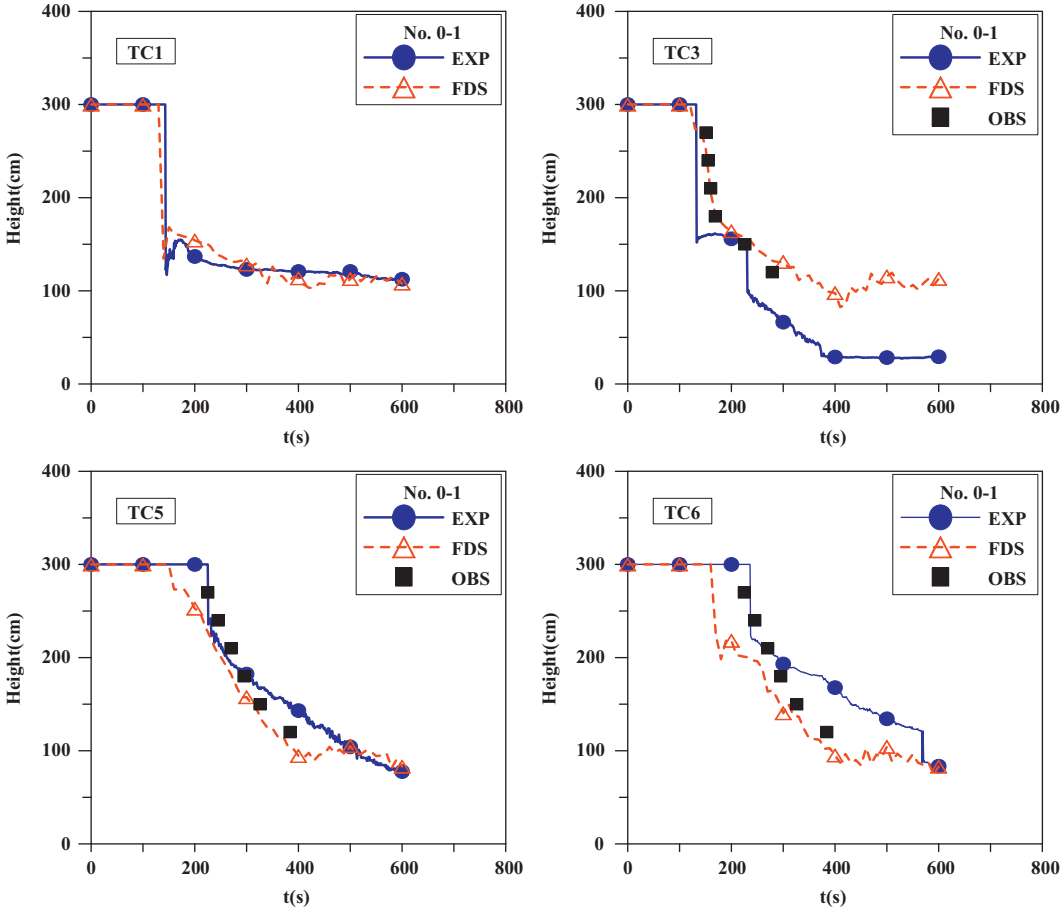

Fig. 11. A comparison of smoke layer descent in No. 0-1.

When the fire was ignited at 2′00″ (120 s), it started to generate large amounts of smoke, which began to descend from the ceiling. At 2′58″(58 s after ignition), the descending smoke was 2 m above the ground and started to flow outdoors through Door1 and into Room2 through Door2. At 3′37″ (217 s), the smoke layer in Room1 descended to 1.5 m; at 5′01″ (301 s), the smoke layer in Room2 was at 1.5 m; and at 5′35″ (335 s), the smoke layer height in Room2 was 1.2 m. At that time, due to the continuous heating of the fire source in Room1, the smoke layer in Room 1 fell to 1.3 m and remained at that level. Finally, at 9′25 (565 s), the smoke layer in Room1 was still at a height of 1.3 m, but the smoke level in Room2 continued to descend below 0.9 m.

A comparison of the FDS simulation and the temperatures (part of the thermocouple tree data) measured in experiment No. 0-1-C, No. 0-2-C and No. 1-1 is shown in Fig. 6. The FDS simulations were conducted before the experiments, so the initial conditions of the two categories were different. Readers can focus on the temperature-rise at each category. However, the different initial states do not affect the results from the *N*-percentage rule. The FDS-simulated temperature-rise at TC1 in No. 0-1-C was roughly the same as that of the experiment, though 2.5 °C average difference existed (at 600 s). The simulated thermocouple tree temperature at TC2 in No. 0-1-C exhibited a relatively large difference from the experimental data because in the FDS simulation, the position of the thermocouple tree TC2 was exactly at the top of the fire source, and so it was heated directly by the fire source. Fearing that the thermocouple would be burnt in the experiment, TC2 was slightly shifted to the side of the fire source. Hence, the largest difference

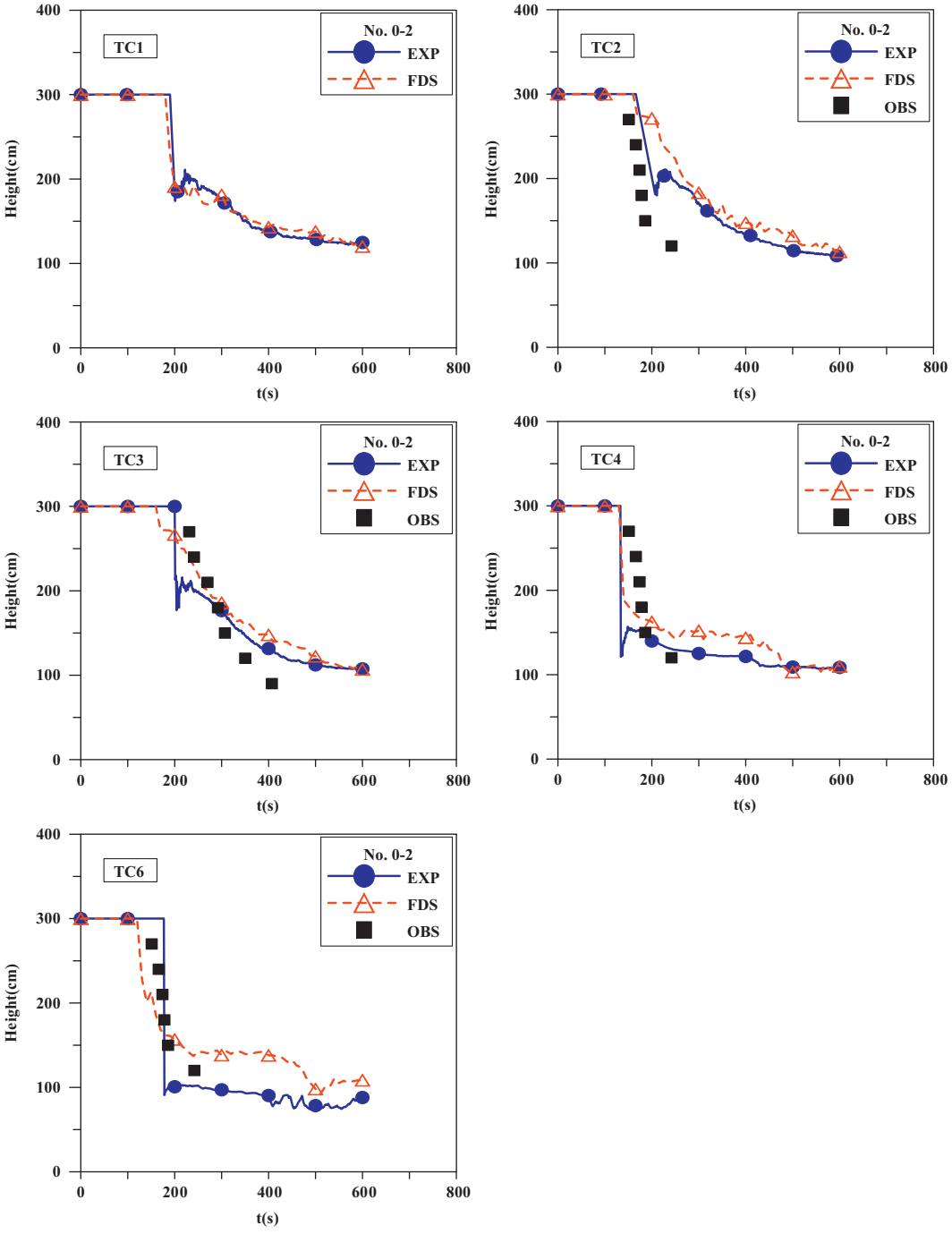

Fig. 12. A comparison of smoke layer descent in No. 0-2.

between the simulation and experimental results was at TC2. In scenario No. 0-2-C, the simulated temperature of TC4 was well-correlated with experimental values, there existed 6.2 °C in average difference (at 600 s).

4.2. The FDS simulation smoke layer descent results

In Figs. 7 and 8, the *N*-percentage rule was used to convert the FDS simulated temperature profiles into smoke layer descent curves. Fig. 7(a) shows the four scenarios with the fire source in Room1. The smoke layer descent curves in the three scenarios without outdoor intake through Door1 (No. 0-1-C, No. 0-1 and No. 1-1) were similar. The smoke layer height was higher in scenario No. 2-1 than in the other three scenarios. The calculated smoke height was nearly identical to the height of the upper frame of the Door1. Fig. 7(b) shows that the scenario No. 0-1-C, with no natural ventilation shaft, had the most rapid smoke layer descent, and the difference between the descent rates in No. 0-1 and No. 1-1 was small. No. 2-1 exhibited larger smoke layer variations.

Fig. 8(b) shows that when the fire was located in Room2, the smoke layer in Room2 descended most rapidly in scenario No. 0-2-C, which had no natural ventilation shaft. The smoke layer height was also lowest in this scenario. Meanwhile, scenarios No. 0-2 and No. 1-2, with a natural ventilation shaft, exhibited reduced speeds of smoke layer descent and higher smoke layer positions. Fig. 8(a) shows that when the fire occurred in Room2, the smoke layer in Room1 descended most rapidly in No. 0-2-C, which had no natural ventilation shaft. The smoke layer height was also lowest in this scenario. Meanwhile, the smoke layer descent was slower in scenarios No. 0-2 and No. 1-2, which included a natural ventilation shaft. In scenario No. 2-2 (with the outdoor wind blowing on Door1), the outdoor wind blowing into the Room1 disperses the smoke layer, creating difficulty in determining the height of the smoke layer.

4.3. Comparison of the FDS simulation smoke layer height results with experimental data

The FDS-simulated temperature, experimental temperature and visual inspection were all used to determine the height of the smoke layer. The results are shown in Figs. 9–16. The symbol EXP in the figures represents experimental data, FDS represents simulation results and OBS represents visually observed results.

4.3.1. No. 0-1-C

A comparison of the measured, observed and simulated smoke layer descents in No. 0-1-C is shown in Fig. 9. The fire source in this scenario was in Room1. Due to the effects of direct burning and thermal radiation on the thermocouple trees TC2 and TC3, the temperature increases at the lower measuring points were caused by the flame and not by fire smoke. This result has been widely recognized [24–27]: in a lower air layer, a thermocouple can measure far higher a temperature than expected [24]. This is due to the influence of radiation emanating from the distant flames and/or the hot gas layer in the environment which can be sensed by the thermocouple. The effective surroundings temperature [24], or mean radiant temperature [25], is much higher than the local gas temperature. Welch et al. [27] explain how to correct the influence of the radiation error on the thermocouple temperature. This is, of course, not what we are exploring in this

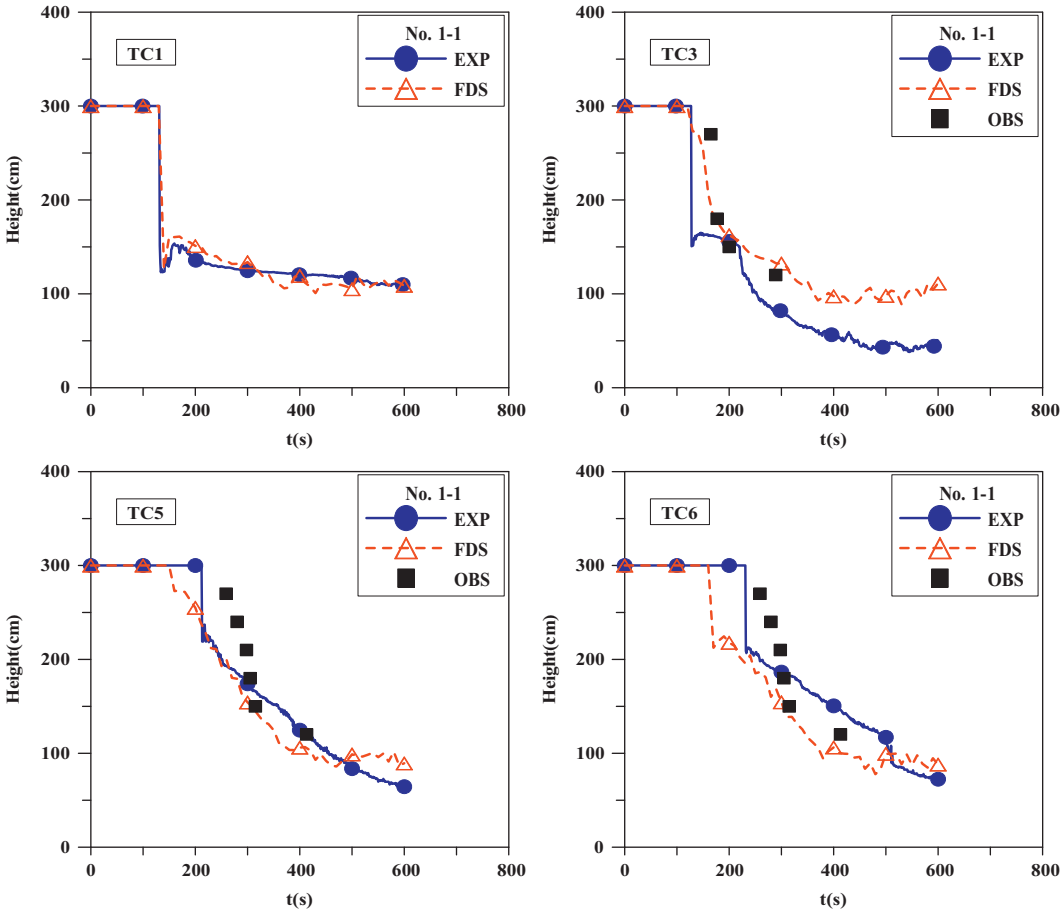

Fig. 13. A comparison of smoke layer descent in No. 1-1.

research, but worthy of further consideration. Therefore, these points (TC2 and TC3 in the No. 0-1-C experiment) are not applicable in the *N*-percentage rule, as the smoke layer descent cannot be determined by the experimental temperatures.

However, the FDS simulation results at TC3 were acceptably consistent with the visually observed data because the thermocouple in FDS was only affected by the smoke layer temperature, not by thermal radiation as in the experiment. In the fire room, the smoke layer height in the FDS simulations can be determined from the thermocouple tree data at greater distances from the fire source. In addition, TC5 and TC6 show that the FDS simulation on smoke height was more accurate in the non-fire room, because thermocouples in the non-fire room are unaffected by the thermal radiation from the fire source.

4.3.2. No. 0-2-C

A comparison of the measured, observed and simulated smoke layer descents in No. 0-2-C is shown in Fig. 10. The fire source was in Room2 in this scenario. TC2 and TC3 were located in the non-fire room. These thermocouples were only subjected to heat from the smoke layer temperature and were not directly affected by the fire sources, so the FDS simulation was quite consistent with the experimental results, and the smoke layer position was also consistent with visual observations. Due to the effects of direct burning and thermal radiation on the thermocouple tree TC5, the temperature (not shown) increases at the lower measuring points were observed. The smoke layer calculated by FDS was slightly higher than the experimentally measured value at TC6, but it still fell within an acceptable range.

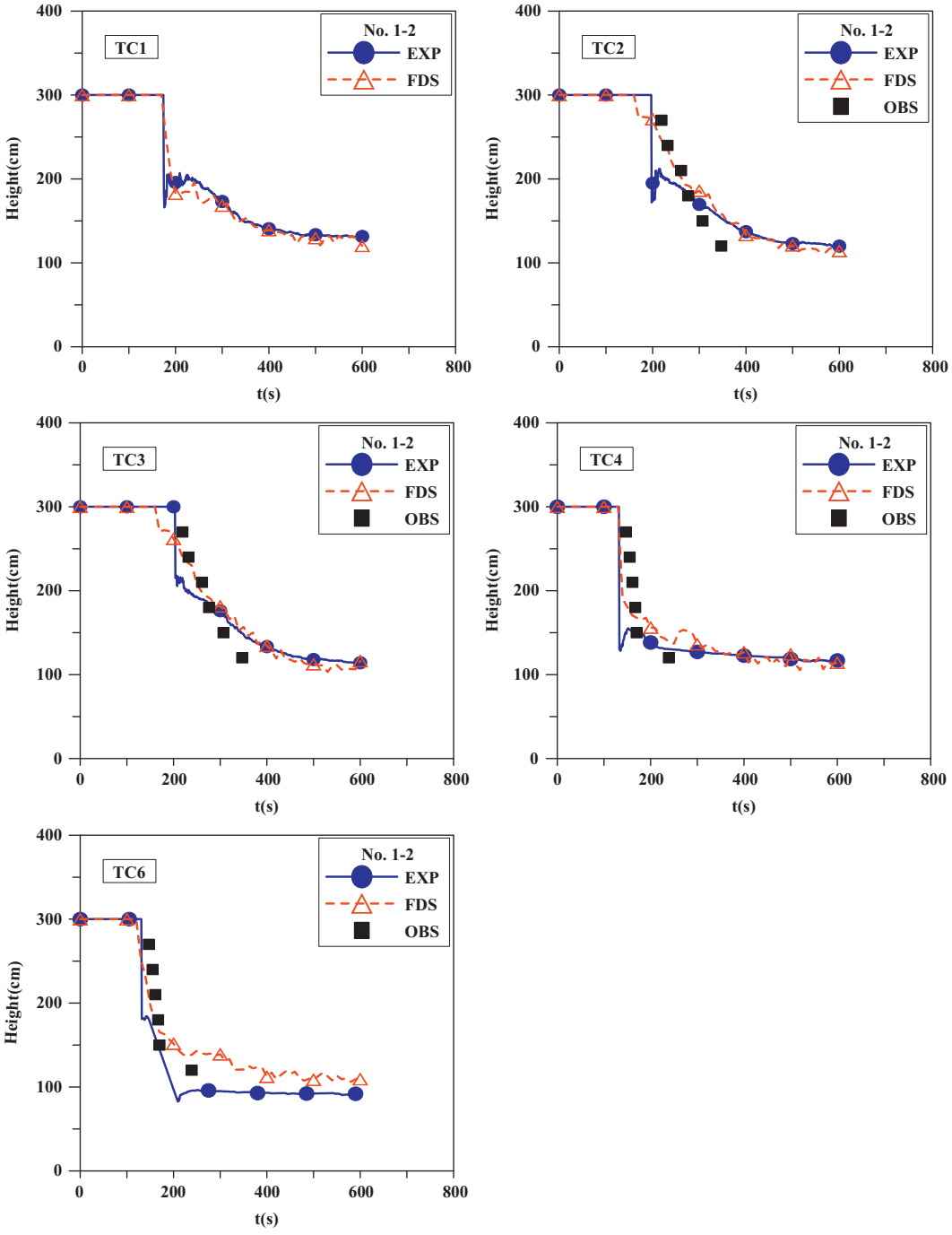

Fig. 14. A comparison of smoke layer descent in No. 1-2.

4.3.3. No. 0-1

A comparison of the measured, observed and simulated smoke layer descents in No. 0-1 is shown in Fig. 11. TC3 was affected by the direct flame and the thermal radiation from the fire source, causing a difference between the simulated and experimentally measured smoke layer heights. From the figure, we can see that the experimentally measured smoke layer descent and the visually detected position of the smoke layer disagree.

According to Sections (a) and (b), the FDS simulation results can be used to determine the smoke layer height. As TC5 was located in the non-fire room, the FDS simulation was able to effectively simulate the smoke layer descent. Because the thermocouple tree TC6 was placed in front of the natural ventilation vent where the smoke layer was affected by smoke exhaust through the vent, the smoke layer temperatures near TC6 were unevenly distributed. The temperature did not decrease in a top-to-bottom manner, making the *N*-percentage rule inaccurate at TC6. The experimental and simulated smoke layer heights from TC6 were, therefore, inconsistent.

4.3.4. No. 0-2

A comparison of the measured, observed and simulated smoke layer descents in No. 0-2 is shown in Fig. 12. The FDS-simulated smoke layer descents measured at TC2 and TC3 (both in the non-fire room) was similar to those in the experimental data, but both were inconsistent with visual observations. This difference arises because when the smoke blew from Room2 to Room1, the smoke had diluted considerably and the temperature of the smoke had already decreased. Then the smoke in Room1 had moved to a lower position. The observers recorded that the smoke layer fell, but the smoke was not hot enough to heat the thermocouple underneath. As a result, the smoke layer height calculated by the *N*-percentage rule was inconsistent with the observed height. At TC6, we can see that the smoke layer descent estimated from the experimental temperatures was inconsistent with that estimated from visual observation due to fire radiation at the thermocouple.

4.3.5. No. 1-1

A comparison of the measured, observed and simulated smoke layer descents in No. 1-1 is shown in Fig. 13. TC5 was unaffected by the fire source, and the FDS result was quite similar to the visual observation and the experimentally measured result. TC6 was located in front of the natural ventilation vent. The smoke temperature at TC6 was affected by the vent flow, resulting in a loss of accuracy in smoke layer determination. In the fire room, the smoke layer curve at TC3 was inconsistent with that from visual observation, due to the effects of direct burning and thermal radiation on the thermocouple tree.

4.3.6. No. 1-2

A comparison of the measured, observed and simulated smoke layer descents in No. 1-2 is shown in Fig. 14. At TC1, TC2 and TC3, the smoke layer positions computed from the FDS temperatures were quite similar to those calculated from experimental temperature measurements, but the visual observations were slightly different. This difference arises because when the smoke blew from Room2 to Room1, some cooler smoke settled to a lower position. The observer thought that the smoke layer had already fallen to the lower position, so the observed position was lower than that determined from

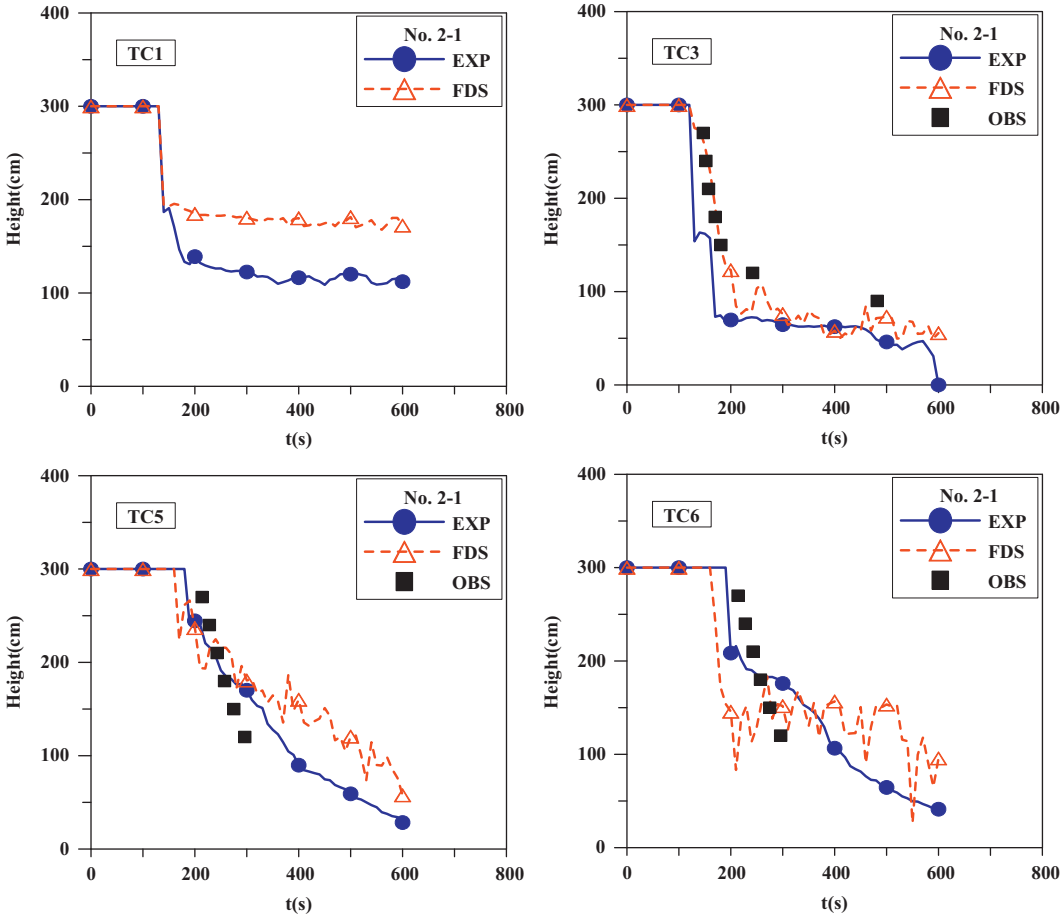

Fig. 15. A comparison of smoke layer descent in No. 2-1.

temperature measurements. Meanwhile, in the fire room, the smoke layer position from FDS simulation of TC4 was similar to those from experimental calculation and visual observation. The temperatures measured by TC4 were not affected by the fire source, which was quite far away. TC6, on the other hand, was affected by the direct burning and thermal radiation in the experiment, and the smoke layer height derived from temperatures measured at TC6 was therefore slightly inconsistent with that from visual observation. The smoke layer descent curve calculated from FDS was quite similar to that observed visually.

4.3.7. No. 2-1

A comparison of the smoke layer descent in No. 2-1 is shown in Fig. 15. In this scenario, the temperature of TC1 was reduced by the outdoor wind that blew toward the interior. At TC3, we can see that the smoke layer position obtained from FDS simulation was close to the visually detected result. At TC5 and TC6 (located on the ventilation flow pathway) in the non-fire room, FDS and experimental results were both unable to show that the smoke layer descended because the wind from outside disturbed the smoke layer, preventing the smoke layer from descending steadily. FDS also yielded strong temperature variations. The honeycomb was not equipped with the fans, so it is possible that the experimental turbulence intensity was high, causing discrepancies and resulting in a loss of accuracy when the *N*-percentage rule was used to determine the smoke layer. Therefore, in scenarios in which outdoor wind blows into the interior, the use of the *N*-percentage rule to determine the smoke layer position is not appropriate.

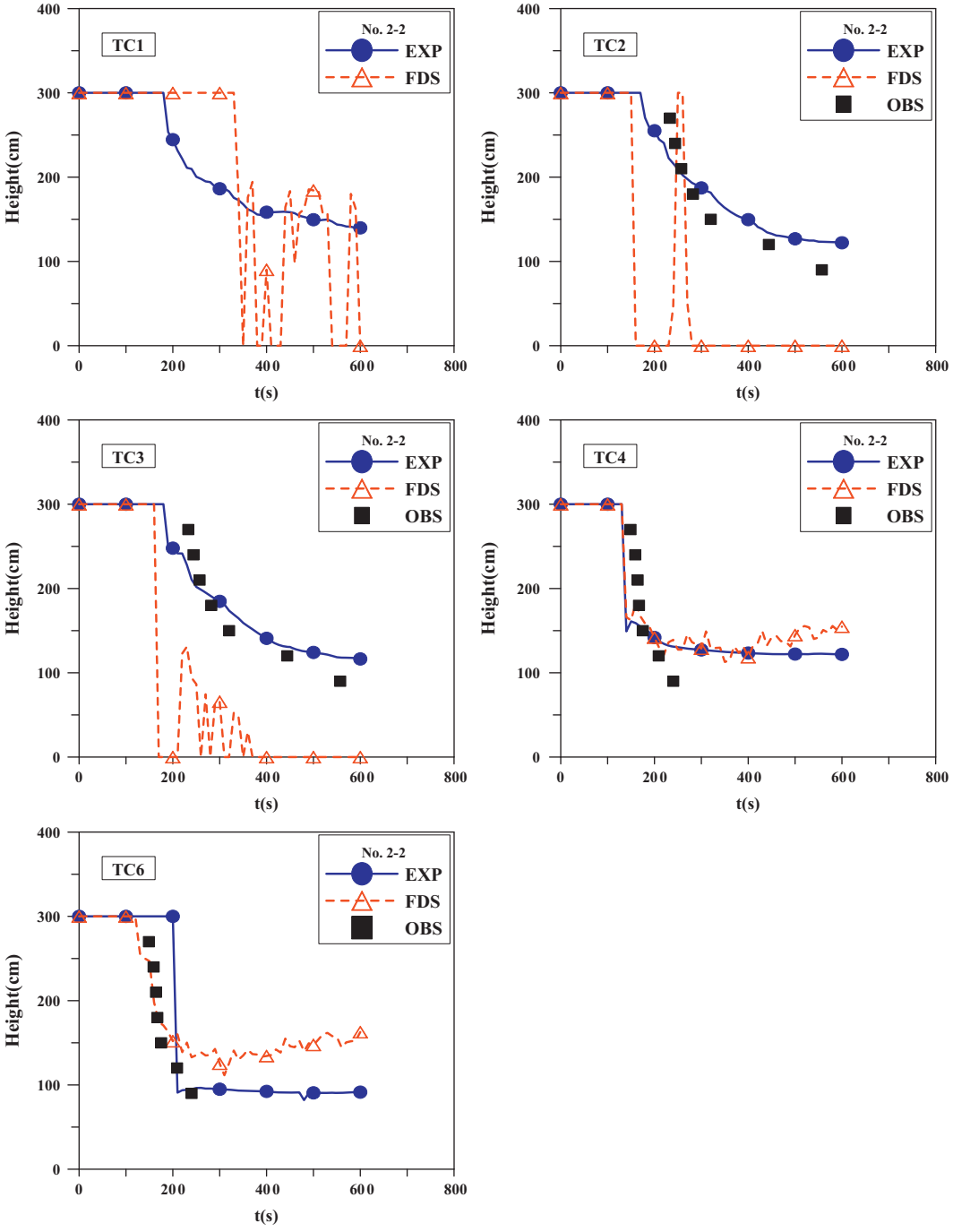

Fig. 16. A comparison of smoke layer descent in No. 2-2.

4.3.8. No. 2-2

A comparison of the smoke layer descent in No. 2-2 is shown in Fig. 16. Because the outside wind would cause a great temperature variation in FDS simulations, the experimental measurements agree better with the observations than the FDS results. The outdoor wind blowing into the Room1 disperses the smoke layer, creating difficulty in determining the smoke layer position. Therefore, the smoke layer position calculated from the measured temperature profiles was still different than the smoke layer that was visually observed.

5. Conclusion

The experimental and FDS simulation results of the spatial layout proposed in this study showed that a room with a natural ventilation shaft can better control the smoke layer from a fire than rooms without a natural ventilation shaft. In the non-fire room, the smoke descent curve determined from the FDS simulated temperatures is consistent with the curve determined from the experimentally measured temperatures and from visual observations. However, in the fire room, the thermocouples are affected by direct burning and fire radiation, and the smoke height cannot be determined from the experimentally measured temperatures. In this case, FDS simulations can be used to compensate for the lack of usable data. In fire scenarios without outdoor wind blowing through the interior, FDS simulations can reliably determine the location of the fire smoke layer. When outdoor air is blown through the interior, the exterior wind causes the smoke layer temperature to be unstable. In these cases, the temperature does not decrease in a top-to-bottom manner, and the *N*-percentage rule is not recommended.

Acknowledgments

Support from the Architecture and Building Research Institute, Ministry of Interior, Taiwan is gratefully acknowledged.

References

[1] W.K. Chow, C.L. Chow, Evacuation with smoke control for atria in green and sustainable buildings, Build. Environ. 40 (2005) 195–200.
[2] H. Chen, N. Liu, W. Chow, Wind effects on smoke motion and temperature of ventilation-controlled fire in a two-vent compartment, Build. Environ. 44 (2009) 2521–2526.
[3] C.A. Short, G.E. Ehittle, M. Owarish, Fire and smoke control in naturally ventilated buildings, Build. Res. Inf. 34 (2009) 23–54.
[4] W.Y. Hung, W.K. Chow, A review on architectural aspects of atrium buildings, Archit. Sci. Rev. 44 (3) (2001) 285–295.
[5] W.K. Chow, Performance of sprinkler in atria, J. Fire Sci. 14 (1996) 466–488.
[6] K.B. McGrattan, S. Hostikka, J.E. Floyd, H.R. Baum, R.G. Rehm, Fire Dynamics Simulator (Version 5), Technical Reference Guide, NIST Special Publication 1018-5, National Institute of Standards and Technology, Gaithersburg, Maryland, 2007.
[7] W.K. Chow, G.W. Zou, Numerical simulation of pressure changes in closed chamber fires, Build. Environ. 44 (2009) 1261–1275.
[8] J.Y. Zhang, W.Z. Lu, R. Huo, R. Feng, A new model for determining neutral-plane position in shaft space of a building under fire situation, Build. Environ. 43 (2008) 1101–1108.
[9] W.K. Chow, G.W. Zou, Correlation equations on fire-induced air flow rates through doorway derived by large eddy simulation, Build. Environ. 40 (2005) 897–906.
[10] X.Q. Sun, L.H. Hu, Y.Z. Li, R. Huo, W.K. Chow, N.K. Fong, Studies on smoke movement in stairwell induced by an adjacent compartment fire, Appl. Therm. Eng. 29 (2009) 2757–2765.
[11] C. Gutiérrez-Montes, E. Sanmiguel-Rojas, A. Viedma, G. Rein, Experimental data and numerical modelling of 1.3 and 2.3 MW fires in a 20 m cubic atrium, Build. Environ. 44 (2009) 1827–1839.
[12] G.W. Zou, W.K. Chow, Evaluation of the field model, fire dynamics simulation, for a specific experimental scenario, J. Fire Prot. Eng. 15 (2005) 77–92.
[13] T.S. Shen, Y.H. Huang, S.W. Chien, Using fire dynamic simulation (FDS) to reconstruct an arson fire scene, Build. Environ. 43 (2008) 1036–1045.
[14] S.C. Kim, H.S. Ryou, An experimental and numerical study on fire suppression using a water mist in an enclosure, Build. Environ. 38 (2003) 1309–1316.
[15] G. Rein, J.L. Torero, W. Jahn, J. Stern-Gottfried, N.L. Ryder, S. Desanghere, Round-robin study of a priori modelling predictions of the Dalmarnock Fire Test One, Fire Saf. J. 44 (2009) 590–602.
[16] G. Rein, C.A. Empis, R. Carvel, The Dalmarnock Fire Tests: Experiments and Modelling, School of Engineering and Electronics, University of Edinburgh, UK, 2007.
[17] V. Babrauskas, Burning Rates. The SFPE Handbook of Fire Protection Engineering, National Fire Protection Association, 1988 (Chapter 3-1).
[18] L.Y. Cooper, M. Harkleoad, J. Quintiere, W. Rinkinen, An Experimental Study of Upper Hot Layer Stratification in Full-Scale Multiroom Fire Scenarios, ASME, 1981.
[19] NFPA 92B. Guide for Smoke Management Systems in Malls, Atria, and Large Areas, 2000.
[20] L. Yi, W.K. Chow, Y.Z. Li, R.A. Huo, Simple two-layer zone model on mechanical exhaust in an atrium, Build. Environ. 40 (2005) 869–880.
[21] T.G. Ma, J.G. Quintiere, Numerical simulation of axi-symmetric fire plumes: accuracy and limitations, Fire Saf. J. 38 (2003) 467–492.
[22] K.B. McGrattan, H.R. Baum, R.G. Rehm, Large Eddy simulations of smoke movement, Fire Saf. J. 30 (1998) 161–178.
[23] J. Kwon, Evaluation of FDS V.4: Upward Flame Spread, Worcester Polytechnic Institute, MA, USA, 2006.
[24] L.G. Blevins, W.M. Pitts, Modelling of bare and aspirated thermocouples in compartment fires gradients, Fire Saf. J. 33 (1999) 239–259.
[25] J. Francis, T.M. Yau, On radiant network models of thermocouple error in pre and post flashover compartment fires, Fire Technol. 40 (2004) 277–294.
[26] S. Broheza, C. Delvosalle, G. Marlair, A two-thermocouples probe for radiation corrections of measured temperatures in compartment fires, Fire Saf. J. 39 (2004) 399–411.
[27] S. Welch, A. Jowsey, S. Deeny, R. Morgan, J.L. Torero, BRE large compartment fire tests-Characterising post-flashover fires for model validation, Fire Saf. J. 42 (8) (2007) 548–567.